Comparison of classical and quantal spectra for the Henon-Heiles potential

1981 J. Phys. A: Math. Gen. 14 L319

(http://iopscience.iop.org/0305-4470/14/9/002)

J. Phys. A: Math. Gen. **14** (1981) L319–L327. Printed in Great Britain

LETTER TO THE EDITOR

Comparison of classical and quantal spectra for the Hénon–Heiles potential

R A Pullen and A R Edmonds

Blackett Laboratory, Imperial College, London SW7 2AZ, England

Received 2 June 1981

Abstract. The quantal energy spectrum is compared with the classical motion for a modified Hénon–Heiles potential. We show that there is good agreement between the amount of classical irregular motion and the proportion of energy eigenvalues sensitive to small changes in the perturbation parameter (as predicted by Percival). We further the work reported by Pomphrey and Noid *et al* by taking into account the full symmetry of the Hamiltonian when computing the eigenvalues, and by showing that most of the high second differences of energy eigenvalues as a function of perturbation parameter correspond to avoided crossings.

1. Introduction

Percival (1973) has predicted that, in the semiclassical limit, the quantal energy spectrum of a dynamical system consists of a regular and an irregular part. In the general case for an inseparable Hamiltonian of N degrees of freedom the regular quantal spectrum corresponds, in the limit $\hbar \to 0$, to regular classical motion, where trajectories lie on N-dimensional invariant toroids. The irregular quantal spectrum corresponds to irregular trajectories which are associated with unstable orbits (Contopoulos 1971) which do not lie on invariant toroids. Energy eigenvalues of the irregular spectrum are more sensitive to a slowly changing or fixed perturbation than those of the regular spectrum. At low energies the classical phase space is dominated by regular trajectories, but as the energy increases a greater volume of phase space is taken up by irregular trajectories.

Other criteria for distinguishing between regular and irregular quantal states have been discussed (e.g. Berry 1977) in terms of the behaviour of the wavefunctions. In the semiclassical limit regular wavefunctions have regular interference fringes and violent fluctuations in intensity associated with caustics of the classical motion. In contrast, irregular states have random patterns of interference maxima and minima with more temperate intensity fluctuations and anticaustics at boundaries of the classical motion.

Pomphrey (1974) and Noid *et al* (1980) have made numerical studies of a modified Hénon–Heiles Hamiltonian (Hénon and Heiles 1964)

$$H = \tfrac{1}{2}(p_x^2 + p_y^2 + x^2 + y^2) + \alpha(x^2 y - \tfrac{1}{3}y^3) \tag{1.1}$$

where $p_x = \dot{x}$, $p_y = \dot{y}$ $(m = 1)$, comparing the quantal spectrum to the classical motion. Pomphrey (1974) found that for $\alpha = 0.088$ there were a number of eigenvalues at higher energies which had large second differences, Δ_i^2, with respect to small variations

in the perturbation parameter, α. Δ_i^2 is given by

$$\Delta_i^2 = |[E_i(\alpha+\Delta\alpha)-E_i(\alpha)]-[E_i(\alpha)-E_i(\alpha-\Delta\alpha)]|. \tag{1.2}$$

These eigenvalues belong to the irregular quantal spectrum and occurred above a critical energy, E_c, which is the energy at which the classical motion begins its transition from being dominated by regular motion to being dominated by irregular motion.

Noid *et al* (1980) made a similar investigation, but with $\alpha = 0.1118$. They identified quantal states as being irregular if, in plots of energy versus perturbation parameter, avoided crossings were observed in the neighbourhood of $\alpha = 0.1118$. They found only one avoided crossing corresponding to two eigenvalues with large second differences. However, their choice of α supported fewer bound states and was further from the semiclassical limit. Full symmetry of the Hamiltonian had not been taken into account and therefore care was needed in distinguishing between large second differences corresponding to avoided crossings and spuriously large second differences produced by crossings. Although Pomphrey (1974) took account of the full symmetry of the Hamiltonian, he only computed non-degenerate eigenvalues which represent about a third of the total number available. We present a more thorough investigation of the same modified Hénon–Heiles Hamiltonian with $\alpha = 0.088$, taking account of the symmetry, and computing all the available eigenvalues up to an energy just below the escape energy. We also show by numerical calculation that most of the large second differences observed correspond to avoided crossings.

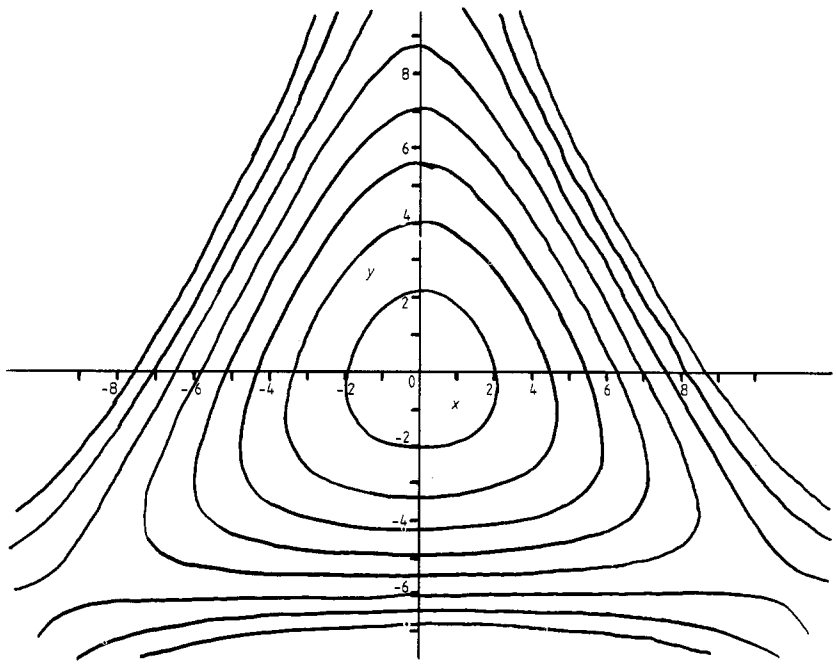

Figure 1. Contour plot for the modified Hénon–Heiles potential with $\alpha = 0.088$.

2. Computation of classical orbits

The classical equations of motion obtained from the Hamiltonian (1.1) are:

$$\ddot{x} = -x - 2\alpha xy \qquad \ddot{y} = -y + \alpha y^2 - \alpha x^2. \tag{2.1}$$

We use the fifth-order error Runge–Kutta–Nyström step method (Henrici 1962, p 173) to compute the classical trajectories with a time step length of 0.1. Tests were made on the accuracy of the computed trajectories by continually checking that the variation in energy was small, and by recomputation with a different step length. Similar methods of computation have been used by the authors for the trajectories of an electron moving simultaneously in a Coulombic and a magnetic field (Edmonds and Pullen 1981) where the equations of motion are more stiffly coupled.

Figure 1 illustrates a contour plot for the Hénon–Heiles potential with $\alpha = 0.088$. The potential has the symmetry of the C_{3v} point group and the bounding curve for energies just below the escape energy at $E = 21.522$ is close to an equilateral triangle.

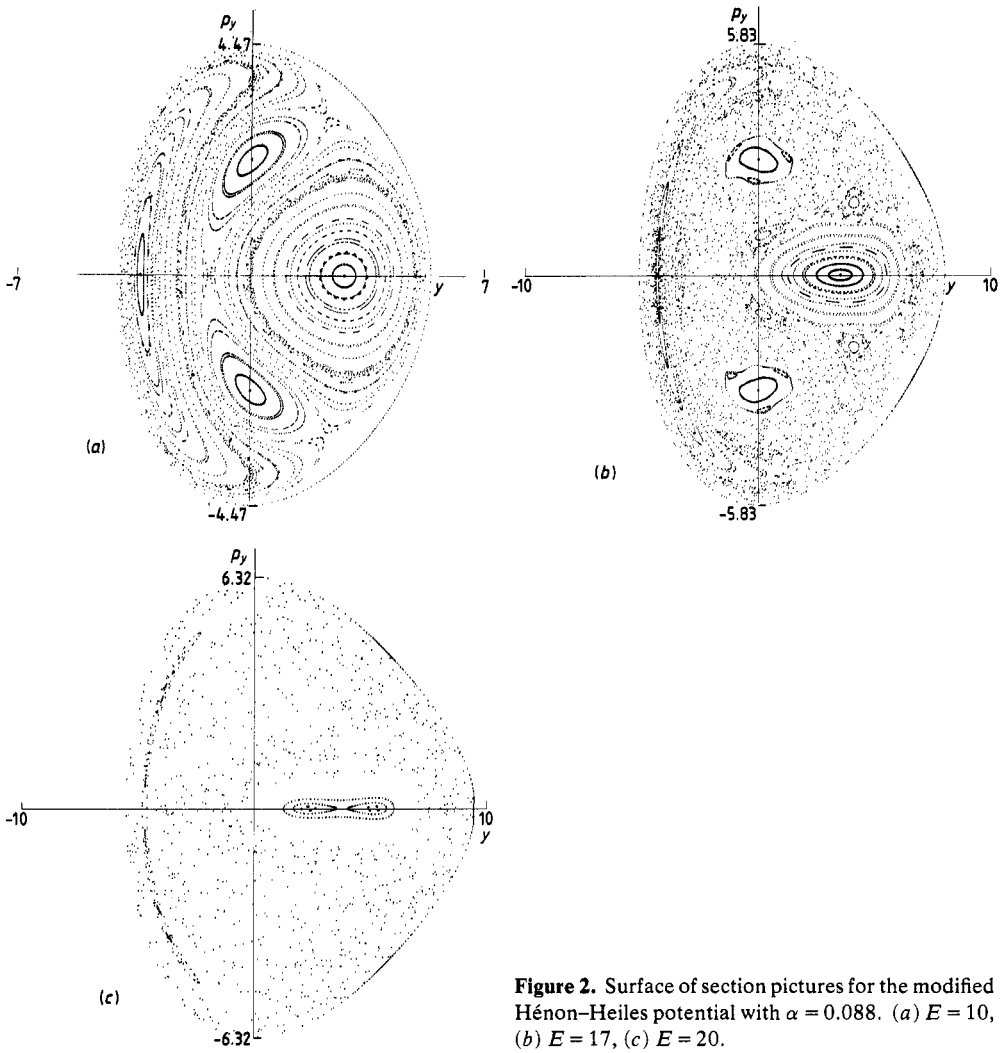

Figure 2. Surface of section pictures for the modified Hénon–Heiles potential with $\alpha = 0.088$. (*a*) $E = 10$, (*b*) $E = 17$, (*c*) $E = 20$.

Surface of section pictures (Poincaré 1897) have been produced (see figures 2(*a*)–(*c*)) for a variety of energies, showing the transition from almost totally regular motion at low energies to almost totally irregular motion at high energies. Conservation of energy restricts any trajectory in 4-dimensional phase space to a 3-dimensional energy shell. At a particular energy, therefore, the restriction $x = 0$ defines a 2-dimensional surface in phase space. Each time a particular trajectory passes through this surface, i.e. each time it crosses the y axis, a point is plotted at the position of intersection (y, p_y). We employ a first-order interpolation process to reduce inaccuracies introduced by using a finite step length.

Regular regions on the surface of section plots are characterised by sets of invariant curves, whereas irregular regions are characterised by a random-like distribution of intersection points. Elliptic points (Arnol'd and Avez 1968, p 218) are clearly seen to exist at $E = 10$ (figure 2(*a*)). These correspond to intersection points of stable periodic orbits, and are located at the centre of a group of invariant curves. At $E = 10$ they occur at $(0, \sqrt{E/2})$, $(0, -\sqrt{E/2})$ and $(2.85, 0)$, $(-3.25, 0)$. The points $(0, \sqrt{E/2})$, $(0, -\sqrt{E/2})$ correspond to trajectories with zero angular momentum which travel up and down two of the reflection symmetry axes of the potential, i.e. along two of the vertices of the equilateral triangle. The surrounding invariant curves are produced by librating-type orbits. The other pair of elliptic points are produced by precessing-type orbits. Both types of orbit are discussed more fully by Noid and Marcus (1977).

As we increase the energy the invariant curves break up, and at high energies where the motion is mainly irregular most trajectories cannot be labelled as being librating-type or precessing-type. At high energies unstable periodic orbits exist which correspond to hyperbolic points (Arnol'd and Avez 1968, p 218) on the surface of section pictures. For example, the elliptic points at $(0, \pm\sqrt{E/2})$ transform to hyperbolic points as we increase the energy from 18 to 19.

In this letter we are not so much concerned with the finer details of the surface of section pictures but we are simply using them to illustrate the transition from a phase space occupied almost wholly by regular trajectories to one occupied almost wholly by irregular trajectories. It should also be noted at this stage that classical details which do not occupy larger volumes of phase space than $(2\pi\hbar)^2$, or areas of $2\pi\hbar$ on surface of section pictures, cannot have a semiclassical significance.

3. Computation of quantal energy spectra

For the purpose of quantum mechanical calculations we consider the Hamiltonian in polar form

$$\hat{H} = -\frac{1}{2}\frac{\partial^2}{\partial r^2} - \frac{1}{2r^2}\frac{\partial^2}{\partial \theta^2} + \frac{1}{2}r^2 + \frac{\alpha r^3}{3}\sin 3\theta \tag{3.1}$$

where $\hbar$ has been put equal to 1. Eigenvalues of this Hamiltonian were calculated by diagonalising the matrix $\tilde{H}$ defined by $\tilde{H}_{ij} = \langle\psi_i|\hat{H}|\psi_j\rangle$, where ψ_i and ψ_j are basis functions which are linear combinations of the eigenfunctions of the unperturbed harmonic oscillator with potential

$$u = \tfrac{1}{2}r^2. \tag{3.2}$$

The normalised eigenfunctions for the potential (3.2) are given by Louck and Shaffer (1960, equation (28)) to be

$$\phi_{Vl} = \frac{1}{\sqrt{2\pi}} R(V, l)\, e^{il\theta} \tag{3.3}$$

where V is zero or a positive integer, and l, the angular momentum quantum number, has allowed values

$$-V, -V+2, -V+4, \ldots, V. \tag{3.4}$$

It is important to take account of the full symmetry of the Hamiltonian for two reasons. Firstly we can divide the matrix $\check{H}$ into submatrices and so reduce computational time and storage, and secondly we can be sure that large second differences calculated by equation (1.2) are due to avoided crossings and not crossings.

The full symmetry group of the Hamiltonian is the C_{3v} point group (which is the symmetry group of the equilateral triangle). There are six elements of this group: E, C_3, C_3^2, σ, σ', σ''. E is the unit element, C_3 and C_3^2 are rotations by 120° and 240° respectively and σ, σ', σ'' are reflections about the vertices of the equilateral triangle (see figure 3). Table 1 is the character table for the irreducible representations of C_{3v}.

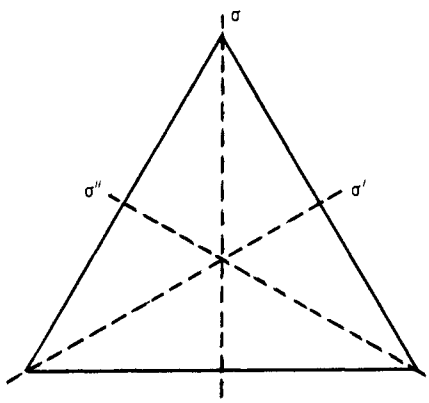

Figure 3. Reflection symmetry axes of the equilateral triangle.

A_1, A_2 and E label the different irreducible representations. We can see immediately from the presence of an irreducible representation of dimension 2 that the perturbation does not completely break the degeneracy of the unperturbed system. We now have eigenstates which are non-degenerate and have A_1 or A_2 symmetry, or we have doubly degenerate states with E symmetry. We choose basis functions which transform according to one or other of the three irreducible representations so that we may

Table 1. Character table of the irreducible representation of the C_{3v} point group.

	E	$2C_3$	3σ
A_1	1	1	1
A_2	1	1	−1
E	2	−1	0

'uncouple' states which belong to different irreducible representations. This follows from the result that matrix elements must be invariant with respect to operations of the symmetry group of the Hamiltonian, and hence matrix elements involving basis functions belonging to different irreducible representations must vanish.

The basis functions we have chosen are linear combinations of the eigenfunctions of the unperturbed harmonic oscillator and transform according to the irreducible representations of C_{3v}:

$$R(V,0),\ R(V,3)\sin 3\theta,\ R(V,6)\cos 6\theta,\ R(V,9)\sin 9\theta,\ R(V,12)\cos 12\theta,\ldots \tag{3.5}$$

$$R(V,3)\cos 3\theta,\ R(V,6)\sin 6\theta,\ R(V,9)\cos 9\theta,\ R(V,12)\sin 12\theta,\ldots \tag{3.6}$$

$$R(V,-2)\,e^{-i2\theta},\ R(V,-1)\,e^{-i\theta},\ R(V,1)\,e^{i\theta},\ R(V,2)\,e^{i2\theta},\ R(V,4)\,e^{i4\theta},\ R(V,5)\,e^{i5\theta}\ldots \tag{3.7}$$

where V must conform to the restriction imposed by (3.4). Basis functions defined by (3.5) transform according to A_1, whilst those defined by (3.6) transform according to A_2, and those defined by (3.7) transform according to E. The matrix formed from basis functions belonging to the E irreducible representation may be split again as matrix elements between functions with angular momentum not differing by 3 vanish, i.e. we may consider the matrix for functions with $l=\ldots-4,-1,2,5\ldots$ separately from the matrix for functions with $l=\ldots-2,1,4,7\ldots$. These matrices give us the same set of eigenvalues and so it is only necessary to compute one of them.

Values of non-zero matrix elements may be calculated using the orthogonality relation

$$\int_0^\infty R(V,l)R(V',l)r\,\mathrm{d}r=\delta_{VV'} \tag{3.8}$$

together with the recursion relation

$$rR(V,l)=-[\tfrac{1}{2}(V+l+2)]^{1/2}R(V+1,l+1)+[\tfrac{1}{2}(V-l)]^{1/2}R(V-1,l+1) \tag{3.9}$$

(Louck and Shaffer 1960, equation (29a)) to obtain

$$\begin{aligned}\int_0^\infty R(V,l+3)\frac{\alpha r^3}{3}R(V',l)r\,\mathrm{d}r=\frac{\alpha}{3}\Bigg[&-\left(\frac{(V'+l+2)(V'+l+4)(V'+l+6)}{8}\right)^{1/2}\delta_{V(V'+3)}\\&+3\left(\frac{(V'+l+2)(V'+l+4)(V'-l)}{8}\right)^{1/2}\delta_{V(V'+1)}\\&-3\left(\frac{(V'+l+2)(V'-l)(V'-l-2)}{8}\right)^{1/2}\delta_{V(V'-1)}\\&+\left(\frac{(V'-l)(V'-l-2)(V'-l-4)}{8}\right)^{1/2}\delta_{V(V'-3)}\Bigg].\end{aligned} \tag{3.10}$$

The radial functions also satisfy the relation

$$R(V,l)=(-1)^lR(v,-l) \tag{3.11}$$

(Louck and Shaffer 1960, equation (38a)) which is required when using linear combinations of the harmonic oscillator eigenfunctions to form our basis functions.

Truncated matrices were diagonalised using the Householder reduction to tri-diagonal form (see Wilkinson and Reinsch 1971, pp 212–6) followed by the method of

bisection (see Wilkinson and Reinsch 1971, pp 249–56). The order of the truncated matrix taken depended on two factors. It was necessary to make the matrix sufficiently large so that the computed eigenvalues would converge to the required precision. However, if we made the matrix too large, the higher eigenvalues would begin to diverge due to the influence of basis functions with a significant proportion of their probability densities outside the 'bounding triangle' of the Hénon–Heiles potential. Due to quantum mechanical tunnelling there are no strictly bound states of the system, though for small excitations the error in assuming discrete eigenstates is small. By truncating our matrix before divergence occurs we are effectively placing a positive infinite potential barrier at the corners of the 'bounding triangle' and hence obtain a discrete spectrum.

For the two matrices representing eigenvalues belonging to the A_1 and A_2 irreducible representations the optimum order for each matrix was found to be 230. This would indicate that the optimum order for the E symmetry matrix should be about 460 (it has about twice the density of eigenvalues of the other matrices). However, storage limitations restricted us to diagonalising matrices up to an order of 400, and so the E

Table 2. Number of regular and irregular states between $E = 14.5$ and $E = 21.5$. For E symmetry states between energies of 19.5 and 21.5 the inaccuracy in the computed eigenvalues was too high to include in the results.

Symmetry matrix	Energy range	Approximate error	No of regular states	No of irregular states	% irregular
A_1	14.5–15.5	10^{-6}	3	0	
A_1	15.5–16.5	10^{-6}	3	0	
A_1	16.5–17.5	10^{-6}	3	0	
A_1	17.5–18.5	2×10^{-5}	4	1	
A_1	18.5–19.5	2×10^{-4}	1	2	
A_1	19.5–20.5	6×10^{-4}	2	2	
A_1	20.5–21.5	2×10^{-3}	1	4	
A_2	14.5–15.5	10^{-6}	3	0	
A_2	15.5–16.5	10^{-6}	0	2	
A_2	16.5–17.5	10^{-6}	3	0	
A_2	17.5–18.5	10^{-6}	1	2	
A_2	18.5–19.5	10^{-6}	3	0	
A_2	19.5–20.5	7×10^{-5}	2	2	
A_2	20.5–21.5	4×10^{-4}	3	1	
E	14.5–15.5	4×10^{-5}	8	4	
E	15.5–16.5	6×10^{-5}	12	0	
E	16.5–17.5	6×10^{-5}	12	0	
E	17.5–18.5	8×10^{-4}	6	8	
E	18.5–19.5	3×10^{-3}	10	4	
E	19.5–20.5	—	—	—	
E	20.5–21.5	—	—	—	
Total	14.5–15.5		14	4	22
Total	15.5–16.5		15	2	12
Total	16.5–17.5		18	0	0
Total	17.5–18.5		11	11	50
Total	18.5–19.5		14	6	30
Total	19.5–20.5		4	4	50
Total	20.5–21.5		4	5	56

symmetry eigenvalues were less accurate than those for A_1 and A_2 symmetry. The accuracy of various eigenvalues is given in table 2. We have considered those eigenvalues computed up to an energy of 21.5 (the escape energy is 21.522).

4. Results and conclusions

The purpose of this letter has been to test the prediction of Percival (1973) that in the semiclassical limit irregular classical motion corresponds to an irregular quantal spectrum. We have identified quantal eigenvalues as being irregular if they have large second differences corresponding to avoided crossings. Table 2 summarises our results. We have used equation (1.2) to compute the second differences for $\Delta\alpha = 0.002$. As the computed eigenvalues are only accurate to a given number of decimal places (table 2 lists the accuracies obtained), the second differences are similarly limited in accuracy. All high second differences listed in table 2, however, were well above this error bound.

As we have taken symmetry into account we would expect all our large second differences to correspond to avoided crossings. This follows from a theorem of von Neumann and Wigner (1929), Teller (1937) and Arnol'd (1978) which forbids crossings between energy levels of the same symmetry for a one-parameter generic real Hamiltonian system. We have checked this numerically for all large second differences obtained. Except for two pairs of eigenvalues all the large second differences clearly correspond to avoided crossings (figure 4 illustrates a sample of avoided crossings). The exceptions are apparent crossings of pairs of eigenvalues associated respectively with states of A_1 and E symmetry. We have decreased the gap in α between successive values of energy computed around the apparent crossings, but limitations in accuracy have not allowed us to identify an avoided crossing. It is likely that the states are very

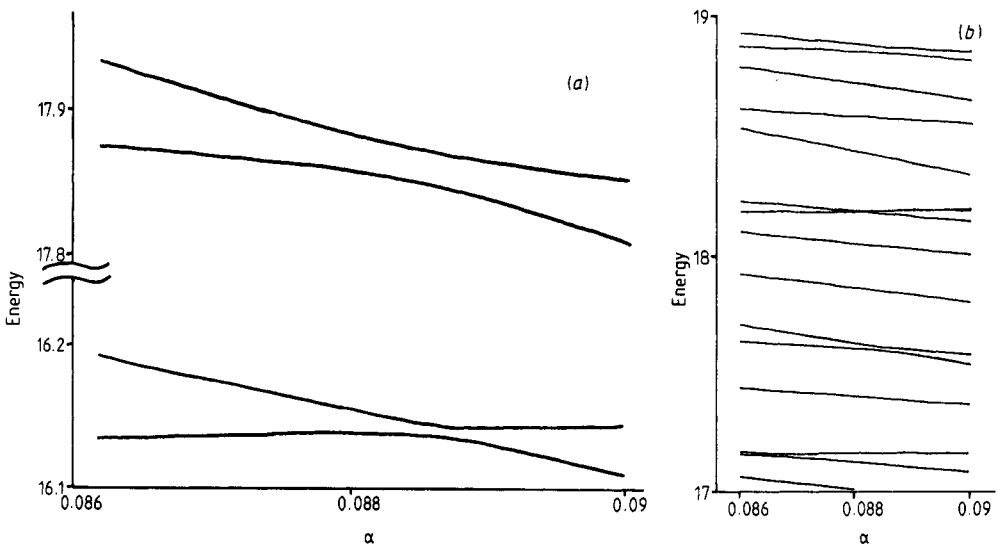

Figure 4. Energy versus perturbation parameter plots. (*a*) illustrates two avoided crossings for A_2 symmetry eignevalues and (*b*) illustrates the E symmetry eigenvalues between energies of 17 and 19.

weakly coupled together, and if we were able to 'magnify' the region around the apparent crossing we would in fact find an avoided crossing.

The results of table 2 show the appearance of irregular quantal states at an energy at which substantial regions of classical phase space become filled with irregular trajectories. As we increase the energy, the proportion of quantal irregular states increases. Of course, our choice of $\hbar$ is quite large, and a smaller value for $\hbar$ would provide a higher density of states and be nearer the semiclassical limit. We might then expect a better correspondence.

In our calculations we have observed the behaviour of the eigenvalues for a small variation in perturbation parameter α. A global picture should be much more informative, i.e. with sufficient computer time we could plot energy against perturbation parameter graphs for large ranges of α and observe the onset of regions of avoided crossings as both E and α increase.

Acknowledgments

We are very grateful to Professor I C Percival for much useful advice during the production of this letter. Also, one of us (RP) would like to thank the Science Research Council for a postgraduate grant.

References

Arnol'd V I 1978 *Mathematical Methods of Classical Mechanics* (New York: Springer) Appendix 10
Arnol'd V I and Avez A 1968 *Ergodic Problems of Classical Mechanics* (New York: Benjamin)
Berry M V 1977 *J. Phys. A: Math. Gen.* **10** 2083–91
Contopoulos G 1971 *Astron. J.* **76** 147–56
Edmonds A R and Pullen R A 1981 *J. Phys. B: At. Mol. Phys.* to be submitted
Hénon M and Heiles C 1964 *Astron. J.* **69** 73–9
Henrici P 1962 *Discrete Variable Methods in Ordinary Differential Equations* (New York: Wiley)
Louck J D and Shaffer W H 1960 *J. Mol. Spectrosc.* **4** 285–97
von Neumann J and Wigner E P 1929 *Z. Phys.* **30** 467–70
Noid D W, Koszykowski M L, Tabor M and Marcus R A 1980 *J. Chem. Phys.* **72** 6169–75
Noid D W and Marcus R A 1977 *J. Chem. Phys.* **67** 559–67
Percival I C 1973 *J. Phys. B: At. Mol. Phys.* **6** L229–32
Poincaré H 1897 *New Methods of Celestial Mechanics* vol 3 ch 27 (Transl NASA Washington DC 1967)
Pomphrey N 1974 *J. Phys. B: At. Mol. Phys.* **7** 1909–15
Teller E 1937 *J. Phys. Chem.* **41** 109–16
Wilkinson J H and Reinsch C 1971 *Handbook for Automatic Computation* (Berlin: Springer)